Cell Reports, Volume *22*

Supplemental Information

GNA11 Q209L Mouse Model Reveals RasGRP3 as an Essential Signaling Node in Uveal Melanoma

Amanda R. Moore, Leili Ran, Youxin Guan, Jessica J. Sher, Tyler D. Hitchman, Jenny Q. Zhang, Catalina Hwang, Edward G. Walzak, Alexander N. Shoushtari, Sébastien Monette, Rajmohan Murali, Thomas Wiesner, Klaus G. Griewank, Ping Chi, and Yu Chen

SUPPLEMENTAL EXPERIMENTAL PROCEDURES

Genetically Engineered Mice

We cloned in human *GNA11*^{Q209L} with an internal glu-glu tag (Van Raamsdonk et al., 2010) into a modified pBTG (Murtaugh et al., 2003) (Addgene plasmid 268) with LoxP sites reversed to remove the forward ATG codon within LoxP site and into Rosa26 locus as previously described (Addgene 15036) (Chen et al., 2013).

Gene targeting was performed at the Rockefeller University Gene Targeting Resource Center (Head: Chingwen Yang). The targeting plasmid was electrophoresed into albino C57BL/6J ES cells and G418 resistant clones were isolated by standard procedures. The clones were screened by Southern blotting. Two positive clones were injected into C57BL/6J blastocysts by the MSKCC Mouse Genetics Core Facility (Head: Willie Mark) and chimeras were mated with albino C57BL/6J females. Germline transmission was confirmed in albino offspring using Southern blotting. For subsequent generations, *GNA11*^{Q209L} mouse genotyping was performed by qPCR of genomic DNA using primers listed in **Table S2**.

Bap1$^{flox/flox}$ (C57BL/6N-Bap1tm1c(EUCOMM)Hmgu/Wtsi) mice were purchased from EUCOMM (LaFave et al., 2015). Tyrosinase-CreERT2 and BRaf^{V600E} mice were obtained from Jackson Labs [B6.Cg-Tg(Tyr-cre/ERT2)13Bos/J (012328); B6.129P2(Cg)-Braftm1Mmcm/J (017837)](Bosenberg et al., 2006). CAG-LSL-EYFP (also known as Ai3) mice (Madisen et al., 2010) were obtained from Jackson Labs [B6.Cg-Gt(ROSA)26Sortm3(CAG-EYFP)Hze/J (007903)]. Standard PCR was performed for genotyping of Tyr-CreERT2, BRaf^{CA}, Bap1$^{flox/flox}$ are listed in Table S2.

Mouse survival was determined under the recommendation of MSKCC veterinary services or upon encountering mice undergoing visible discomfort and in accordance to the MSKCC Institutional Animal Care and Use Committee (IACUC 11-12-029). In accordance to our animal protocol, mice were euthanized in response but not limited to the following: tumors larger than 1cm^3, tumor ulceration, tumors located too close to the trunk of the mice to impeded movement and blood flow and tumor burden.

Intraperitoneal injection of tamoxifen was performed at 4-weeks of age with no regard to the sex of the animals and histology was similar between both males and females.

Allograft and Treatment

Tumors from *Tyr-CreER*^{T2};*Braf*^{V600E};*Bap1*^{KO} and *Tyr-CreER*^{T2};*GNA11*^{Q209L};*Bap1*^{KO} mice were expanded in 6-8 week old C.B17-scid mice (C.B-*Igh-1*^{b}/IcrTac-*Prkdc*^{scid}; Taconic) and then serial grafted bilaterally using equal size tumors. The experimental cohort of mice 6-8 week old female C.B17-scid mice (Taconic) of 8 tumors for the vehicle and trametinib treated *Tyr-CreER*^{T2};*GNA11*^{Q209L};*Bap1*^{KO} and 24 tumors for the trametinib treated arm and 7 tumors for the control arm for *Tyr-CreER*^{T2};*Braf*^{V600E};*Bap1*^{KO} tumors. The size of each cohort was determined on the basis of previous experiments without specific statistical methods. Mice we treated with 3mg kg^{-1} trametinib (Active Biochem) dissolved in trametinib solvent (30% PEG-400, 0.5% TWEEN® 80, 5% propylene glycol in PBS) once daily for 5 days a week. Tumors were measured with calipers every 2 or 3 days for up to 25 days with trametinib treatment and were actively measured for at least 10 days before treatment. Tumor growth curves were visualized with Prism GraphPad 6.0. Tumor volume was calculated using the formula: $\text{volume} = \frac{\pi(length)(width)(height)}{6}$.

Histology and immunohistochemistry

Prior to immunohistochemistry, melanin bleaching was performed using a delicate melanin bleach kit (Polysciences Inc.) according to the manufacturer's instructions. Immunohistochemistry for HMB45, DT101, BC199 melanoma cocktail (Abcam, ab732, 1:50), MITF (Cell Signaling Technology, 12590, 1:50), Ki-67 (Abcam, ab16667, 1:100) antibodies were diluted in SignalStain antibody diluent (Cell Signaling Technology). Staining was performed using a standard multimer/diaminobenzidine (DAB) detection protocol for MITF and Ki67 and red chromogen staining (alkaline phosphatase; Ventana; UltraMap Red) for the melanoma cocktail following epitope retrieval with citrate (Ventana; CC1), hematoxylin counterstain on a Discovery Ultra system (Roche/Ventana) with appropriate negative and positive controls. Immunohistochemistry for each tissue shown was preformed on tissues harvested from at least 5 animals.

Immunofluorescence of eye and skin

All tissues were fixed at room temperature for 30min in 4% paraformaldehyde (Electron Microscopy Sciences). Tissues were then incubated in 30% sucrose in PBS at 4°C overnight, washed once with PBS, embed in OCT, flash frozen and cut into 5 µM sections using a cryostat. Tissue sections were blocked for 1 hour using 5% goat serum, incubated with Gp100 antibody at 4 °C overnight and secondary antibody for 2 hours at room temperature. Slides were mounted using PBS with 1ug ml^{-1} DAPI for direct visualization of YFP and Gp100. Images were taken on a Nikon Eclipse TE2000-E microscope using a Photometric Coolsnap HQ camera. Images were taken with ×20 (numerical aperture 0.75) objectives. Monochrome images taken with DAPI, YFP and Texas Red filter sets were pseudo-colored blue, green and red, respectively, and merged using ImageJ.

Intraperitoneal injection of tamoxifen was administered in both sexes of the animals and histology was similar between both males and females. At least 45 animals for each genotype ($GNA11^{Q209L}$, $GNA11^{Q209L}$; $Bap1^{lox/lox}$, $Bap1^{lox/lox}$, $BRaf^{V600E}$; $Bap1^{lox/lox}$) were injected with tamoxifen and observed. At least 14 animals for each genotype underwent a full necropsy and were tissues evaluated by H&E.

RNA-seq

For mouse tumors, total RNA was extracted from fresh-frozen tissue or cell lines using Qiagen's RNeasy Mini Kit (Qiagen). The isolated RNA was processed for RNA-sequencing by the Integrated Genomics Core Facility at MSKCC. The libraries were sequenced on an Illumina HiSeq-2500 platform with 51 bp paired-end reads to obtain a minimum yield of 40 million reads per sample. The sequence data were mapped to the mouse reference genome (mm9) and the number of reads was quantified using STAR v2.330 (Dobin et al., 2013).

For UPMM3 cells, the libraries were sequenced on an Illumina HiSeq-2500 platform with 51 bp single-end reads to obtain a minimum yield of 40 million reads per sample. The sequence data were mapped to the human reference genome (hg19) and the number of reads was quantified using Cufflinks (Roberts et al., 2011). GSEA was performed using JAVA GSEA 2.0 program (Subramanian et al., 2005). The gene sets used for analysis were the Broad Molecular Signatures Database gene sets c2 (curated gene sets), c5 (gene ontology gene sets), c6 (oncogenic signatures). GSEA enrichment sets are shown in **Table S1**.

Level 3 RNA-seqV2 data for TCGA uveal melanoma (n=80) and cutaneous melanoma (SKCM; n=471) were downloaded from NIH TCGA server. We merged the samples and annotated them by mutational status ($BRAF^{V600E}$, GNAQ or GNA11 at R183 or Q209) and by tissue source (primary or metastatic). Differential gene expression was performed using ANOVA analysis with the Partek Genomics Suite 6.6 in both the TCGA and genetically engineered mouse model datasets. Expression of RASGRP3 from pan-TCGA cancers was downloaded from cBioportal (Cerami et al., 2012) and from Gene Expression across Normal and Tumor tissue (GENT) (Shin et al., 2011) was downloaded from http://medicalgenome.kribb.re.kr/GENT/.

Ki-67 quantification

Following immunohistochemistry for Ki-67, 10 randomly selected field images at 40 x magnifications were taken. These images were converted to greyscale, threshold adjusted, and particles were analyzed using ImageJ v1.60 (NIH) automated counting to determine the number of cells per field. The same parameters were used throughout quantification. To determine the percent of cells that were positive for Ki-67, we performed identical procedures while optimizing the threshold to include only cells with positive DAB staining. The same parameters were used throughout quantification.

PCR for Bap1 lox/lox excision

DNA from Bap1 mice was isolated using DNeasy Blood & Tissue Kit (Qiagen). DNA from whole cutaneous tumors and dissected uveal tracts were used for the PCR. Control tissues were isolated from mouse toes. PCR of genomic DNA was performed using primers listed in **Table S2**.

Cell lines

Melan-a cells were provided by D. Bennett (St. George's Hospital, University of London, London, UK)(Bennett et al., 1987) and were grown in RPMI with 200nM 12-O-Tetradecanoylphorbol-13-Acetate (TPA; Sigma-Aldrich) before stable expression. Melan-a cells stably expressing $GNAQ^{Q209L}$, $BRAF^{V600E}$ and $KRAS^{G12V}$ were propagated in the absence of TPA. MEL202, MEL270, OMM1.3, COLO800 cells were grown in RPMI. UPMD1, UPMD2 and UPMM3 cells were grown in Ham's F12 media. A375 and A2058 cells were grown in DMEM media. 293T cells were used for retrovirus and lentivirus production and maintained in DMEM media. All cell culture media contained 10% FBS, penicillin (100 U ml^{-1}), streptomycin (100 µg ml^{-1}), L-glutamine (2mM). All cells were grown in a humidified incubator at 37 °C with 5% CO_2 and were tested regularly for mycoplasma contamination. All cell lines used were negative for mycoplasma. All uveal melanoma cell lines were validated for mutations status by MSK-IMPACT.

Proliferation and survival assays

Growth curves were performed following shRNA infection and around 1,000–3,000 cells were plated in a 96-well plate 24 hours following infection. Every 48 hours following infection, the number of cells was determined using a CelltiterGlo assay (Promega). IC_{50} assays were performed by plating 1,000–3,000 cells in a 96-well plate, allowed to adhere overnight, and then incubated with either fresh media containing trametinib. After 5 days, the number of cells was determined using a CelltiterGlo assay. Representative experiments are shown. Cell growth was assessed in three independent experiments, each in quadruplet.

Immunoblotting

Whole cell lysates were prepared in cell lysis buffer (Cell Signaling Technology) containing freshly added protease and phosphatase inhibitors (PhosSTOP, Roche, cOmplete EDTA-Free, Roche). Tumor lysates were generated by homogenization of flash-frozen tissue in cell lysis buffer (Cell Signaling Technology) containing freshly added protease and phosphatase inhibitors (PhosSTOP, Roche, cOmplete EDTA-Free, Roche). Equal amounts of protein, as measured by BCA protein assay (Thermo Scientific), were resolved on NuPAGE Novex 4-12% Bis-Tris Protein Gels (Life Technologies) and transferred electrophoretically onto a 0.45µm nitrocellulose membrane (Bio-Rad). Membranes were blocked for 1 hour at room temperature in StartingBlock TBS (Thermo Scientific) or Odyssey blocking buffer (LI-COR) before being incubated overnight at 4°C with the primary antibodies diluted at 1:1000 unless otherwise noted in either StartingBlock or Odyssey blocking buffer. The following primary antibodies were used (Cell Signaling unless noted otherwise): phospho-p44/42 MAPK (Erk1/2) (Thr202/Tyr204; 4370), p44/42 MAPK (Erk1/2;4695), phospho-$P90^{RSK}$ (Ser380;12032), RSK1/2/3 (9355), RasGRP3 (3334), Ras (8832), CyclinD1 (2922), SPRY4 (Santa Cruz Biotechnology; sc-30051), BAP1 (Santa Cruz Biotechnology; sc-28383), HA-tag (Roche; 3F10), GNAQ (abcam; ab199533), GAPDH (1:5,000

dilution; Applied Biological Materials, G041), β-actin (1:5,000 dilution; abcam, AC15). The Ras-GTP assay was performed according to manufactures instructions (Cell Signaling; 8821).

shRNA and inhibitors

For shRNA mediated knockdown of RASGRP3 the following hairpins were used with sequences listed in **Table S3**. Human shRASGRP3-1 and shRASGRP3-2 were obtained from the MSKCC RNAi Core in pLKO.1 and were subcloned into Tet-pLKO-puro (Wiederschain et al., 2009) (Addgene plasmid 21915). Mouse shRasgrp3-1 and shRasgrp3-2 were obtained from the MSKCC RNAi Core in pLKO.1. Stable expressing Tet-ON shRasGRP3 were induced with doxycycline 1μg ml^{-1} (Research Products International) and cells were harvested for protein 72 hours post-doxycycline addition. Melan-a cells were treated with the indicated dose of trametinib (SelleckChem). Cell growth for the half-maximal inhibitory concentration (IC_{50}) was assessed using CellTiter-Glo (Promega) five days post trametinib treatment.

Exogenous gene expression

Melan-a cells were stably transduced with: BRAF V600E, MSCV-HA-FLAG-BRAF-V600E. MSCV-HA-FLAG-V600E was cloned using the gateway method using pDONOR-BRAF (Addgene plasmid 70300) and subcloned into MSCV-HA-FLAG-puro-Dest. Site directed mutagenesis was performed using QuikChange (Agilent) to wild-type *BRAF* to introduce a p.Val600Glu mutation to give $BRAF^{V600E}$. KRAS G12V: MSCV-GFP-KRAS G12V, KRAS G12V (Addgene plasmid 31200) (Yang et al., 2011) was subcloned into MSCV-IRES-GFP-Dest using the gateway method. GNAQ Q209L: MSCV-puro-GNAQ Q209L, cDNA for the wild-type human *GNAQ* was obtained from Origene (sc128110) and cloned into MSCV-puro (Addgene plasmid 24828)(Olive et al., 2009). Site directed mutagenesis was performed using QuikChange (Agilent) to wild-type *GNAQ* to introduce a p.Gln209Leu mutation to give $GNAQ^{Q209L}$. QuikChange primers are listed in **Table S2**. The sequences of all constructs were confirmed by Sanger sequencing.

Resource Table

REAGENT or RESOURCE	SOURCE	IDENTIFIER
Antibodies		
Rabbit monoclonal anti-phospho-p44/42 MAPK (Erk1/2) (Thr202/Tyr204)	Cell Signaling Technology	Cat#4370; RRID: AB_2315112
Rabbit monoclonal anti-p44/42 MAPK (Erk1/2)	Cell Signaling Technology	Cat#4695; RRID: AB_390779
Rabbit monoclonal anti-Phospho-p90RSK (Ser380)	Cell Signaling Technology	Cat#;12032
Rabbit monoclonal anti-RSK1/RSK2/RSK3	Cell Signaling Technology	Cat#9355; RRID: AB_659900
Rabbit monoclonal anti-RASGRP3	Cell Signaling Technology	Cat#3334; RRID: AB_2269292
Mouse monoclonal anti-RAS	Cell Signaling Technology	Cat#8832
Rat monoclonal anti-HA (hemagglutinin)	Roche	Cat#3F10; RRID: AB_2314622
Rabbit monoclonal anti-GNAQ	Abcam	Cat#ab199533
Mouse monoclonal anti-BAP1 (C-4)	Santa Cruz Biotechnology	Cat# sc-28383; RRID:AB_626723
Rabbit monoclonal anti-Ki67 [SP6]	Abcam	Cat# ab16667, RRID:AB_302459
Rabbit monoclonal anti-MITF	Cell Signaling Technology	Cat# 12590, RRID:AB_2616024
Rabbit polyclonal anti-SPRY4	Santa Cruz Biotechnology	Cat# sc-30051 RRID:AB_2195449
Rabbit monoclonal anti-CyclinD1	Cell Signaling Technology	Cat# 2922 RRID:AB_2228523

Rabbit monoclonal anti-Melanoma gp100	Abcam	Cat#ab137078
Mouse monoclonal anti-Melanoma antibody [HMB45 + DT101 + BC199]	Abcam	Cat# ab732, RRID:AB_305844
Biological Samples		
Genetically engineered mouse tissues	This paper	N/A
Chemicals, Peptides, and Recombinant Proteins		
Trametinib (GSK1120212; mouse treatment)	Active Biochem	Cat#: A-1258; CAS: 871700-17-3
Trametinib (GSK1120212; cell treatment)	Selleck Chemicals	S2673; CAS: 871700-17-3
Critical Commercial Assays		
Ras-GTP	Cell Signaling Technology	Cat#8821
CellTiterGlo	Promega	G9242
Deposited Data		
Raw and analyzed RNA-sequencing data	This paper	GEO: GSE97225
Mendeley raw data	This paper	doi:10.17632/g2v849vzzm doi:10.17632/my5g8mdrkg doi:10.17632/8r58nb2ttc
Experimental Models: Cell Lines		
Mouse: Melan-a	(Bennett et al., 1987)	Wellcome Trust Functional Genomics Cell Bank; RRID:CVCL_4624
Human: MEL202	(Griewank et al., 2012)	RRID:CVCL_C301
Human: MEL270	(Griewank et al., 2012)	RRID:CVCL_C302
Human: UPMD2	(Griewank et al., 2012)	RRID:CVCL_C298
Human: OMM1.3	(Griewank et al., 2012)	RRID:CVCL_C306
Human: UPMM3	(Griewank et al., 2012)	RRID:CVCL_C295
Human: UPMD1	(Griewank et al., 2012)	RRID:CVCL_C297
Human: A375	ATCC	CRL-1619; RRID:CVCL_0132
Human: A2058	ATCC	CRL-11147; RRID:CVCL_1059
Human: COL800	Sigma-Aldrich	93051123; RRID:CVCL_1135
Experimental Models: Organisms/Strains		
Mouse: Tyr::CreER^{T2}: B6.Cg-Tg(Tyr-cre/ERT2)13Bos/J	The Jackson Laboratory	RRID:IMSR_JAX:012328
Mouse: BRaf^{CA}: B6.129P2(Cg)-*Braf*^{tm1Mmcm}/J	The Jackson Laboratory	RRID:IMSR_JAX:017837
Mouse: Bap1$^{flox/flox}$: Bap1$^{tm1a(EUCOMM)Hmgu}$	(LaFave et al., 2015)	RRID:MGI:5550605
Mouse: GNA11^{Q209L} (R26-LSL-GNA11_Q209L)	This paper	N/A
Mouse: CB17-SCID: C.B-*Igh-1*^{b}/IcrTac-*Prkdc*^{scid}	Taconic	RRID:IMSR_TAC:cb17sc
Mouse: R26-LSL-EYFP (B6.Cg-*Gt(ROSA)26Sor*$^{tm3(CAG-EYFP)Hze}$/J)	The Jackson Laboratory	RRID: IMSR_JAX: 007903
Oligonucleotides		

Primers; see Table S2	This paper	N/A
shRNA targeting RasGRP3; see Table S3	The RNAi Consortium ShRNA Library	MSKCC RNAi Core
Recombinant DNA		
MSCV-BRAF-V600E-HA-FLAG	This paper	Quikchange; Gateway; MSCV-HA-FLAG-puro-Dest
R777-E016 Hs.BRAF-nostop	Addgene	Addgene Plasmid #70300
MSCV-K-RAS-G12V-GFP	This paper	Gateway; MSCV-IRES-GFP-Dest
pDONR223-K-RAS V12	(Yang et al., 2011)	Addgene Plasmid #31200
GNAQ cDNA	Origene	sc128110
pBTG	(Murtaugh et al., 2003)	Addgene Plasmid #268
pRosa26PAm1	(Chen et al., 2013; Murtaugh et al., 2003)	Addgene Plasmid #15036
MSCV-puro	(Olive et al., 2009)	Addgene Plasmid #24828
MSCV-puro-GNAQ-Q209L	This paper	Quikchange; MSCV-puro
Software and Algorithms		
STAR v2.330	(Dobin et al., 2013)	
GSEA		http://software.broadinstitute.org/gsea/index.jsp
GraphPad Prism v6.0		https://www.graphpad.com/scientific-software/prism/
Partek Genomics Suite		http://www.partek.com/pgs
Cufflinks	(Roberts et al., 2011)	

Supplementary References

Bennett, D.C., Cooper, P.J., and Hart, I.R. (1987). A line of non-tumorigenic mouse melanocytes, syngeneic with the B16 melanoma and requiring a tumour promoter for growth. Int J Cancer *39*, 414-418.

Bosenberg, M., Muthusamy, V., Curley, D.P., Wang, Z., Hobbs, C., Nelson, B., Nogueira, C., Horner, J.W., Depinho, R., and Chin, L. (2006). Characterization of melanocyte-specific inducible Cre recombinase transgenic mice. Genesis (New York, NY : 2000) *44*, 262-267.

Cerami, E., Gao, J., Dogrusoz, U., Gross, B.E., Sumer, S.O., Aksoy, B.A., Jacobsen, A., Byrne, C.J., Heuer, M.L., Larsson, E., *et al.* (2012). The cBio cancer genomics portal: an open platform for exploring multidimensional cancer genomics data. Cancer discovery *2*, 401-404.

Chen, Y., Chi, P., Rockowitz, S., Iaquinta, P.J., Shamu, T., Shukla, S., Gao, D., Sirota, I., Carver, B.S., Wongvipat, J., *et al.* (2013). ETS factors reprogram the androgen receptor cistrome and prime prostate tumorigenesis in response to PTEN loss. Nature medicine *19*, 1023-1029.

Dobin, A., Davis, C.A., Schlesinger, F., Drenkow, J., Zaleski, C., Jha, S., Batut, P., Chaisson, M., and Gingeras, T.R. (2013). STAR: ultrafast universal RNA-seq aligner. Bioinformatics *29*, 15-21.

Griewank, K.G., Yu, X., Khalili, J., Sozen, M.M., Stempke-Hale, K., Bernatchez, C., Wardell, S., Bastian, B.C., and Woodman, S.E. (2012). Genetic and molecular characterization of uveal melanoma cell lines. Pigment cell & melanoma research *25*, 182-187.

LaFave, L.M., Beguelin, W., Koche, R., Teater, M., Spitzer, B., Chramiec, A., Papalexi, E., Keller, M.D., Hricik, T., Konstantinoff, K., *et al.* (2015). Loss of BAP1 function leads to EZH2-dependent transformation. Nature medicine *21*, 1344-1349.

Madisen, L., Zwingman, T.A., Sunkin, S.M., Oh, S.W., Zariwala, H.A., Gu, H., Ng, L.L., Palmiter, R.D., Hawrylycz, M.J., Jones, A.R., *et al.* (2010). A robust and high-throughput Cre reporting and characterization system for the whole mouse brain. Nat Neurosci *13*, 133-140.

Murtaugh, L.C., Stanger, B.Z., Kwan, K.M., and Melton, D.A. (2003). Notch signaling controls multiple steps of pancreatic differentiation. Proceedings of the National Academy of Sciences of the United States of America *100*, 14920-14925.

Olive, V., Bennett, M.J., Walker, J.C., Ma, C., Jiang, I., Cordon-Cardo, C., Li, Q.J., Lowe, S.W., Hannon, G.J., and He, L. (2009). miR-19 is a key oncogenic component of mir-17-92. Genes & development *23*, 2839-2849.

Roberts, A., Trapnell, C., Donaghey, J., Rinn, J.L., and Pachter, L. (2011). Improving RNA-Seq expression estimates by correcting for fragment bias. Genome biology *12*, R22.

Shin, G., Kang, T.W., Yang, S., Baek, S.J., Jeong, Y.S., and Kim, S.Y. (2011). GENT: gene expression database of normal and tumor tissues. Cancer Inform *10*, 149-157.

Subramanian, A., Tamayo, P., Mootha, V.K., Mukherjee, S., Ebert, B.L., Gillette, M.A., Paulovich, A., Pomeroy, S.L., Golub, T.R., Lander, E.S., *et al.* (2005). Gene set enrichment analysis: a knowledge-based approach for interpreting genome-wide expression profiles. Proceedings of the National Academy of Sciences of the United States of America *102*, 15545-15550.

Van Raamsdonk, C., Griewank, K., Crosby, M., Garrido, M., Vemula, S., Wiesner, T., Obenauf, A., Wackernagel, W., Green, G., Bouvier, N., *et al.* (2010). Mutations in GNA11 in uveal melanoma. The New England Journal of Medicine *363*, 2191-2199.

Wiederschain, D., Wee, S., Chen, L., Loo, A., Yang, G., Huang, A., Chen, Y., Caponigro, G., Yao, Y.-M.M., Lengauer, C., *et al.* (2009). Single-vector inducible lentiviral RNAi system for oncology target validation. Cell cycle (Georgetown, Tex) *8*, 498-504.

Yang, X., Boehm, J.S., Yang, X., Salehi-Ashtiani, K., Hao, T., Shen, Y., Lubonja, R., Thomas, S.R., Alkan, O., Bhimdi, T., *et al.* (2011). A public genome-scale lentiviral expression library of human ORFs. Nature methods *8*, 659-661.

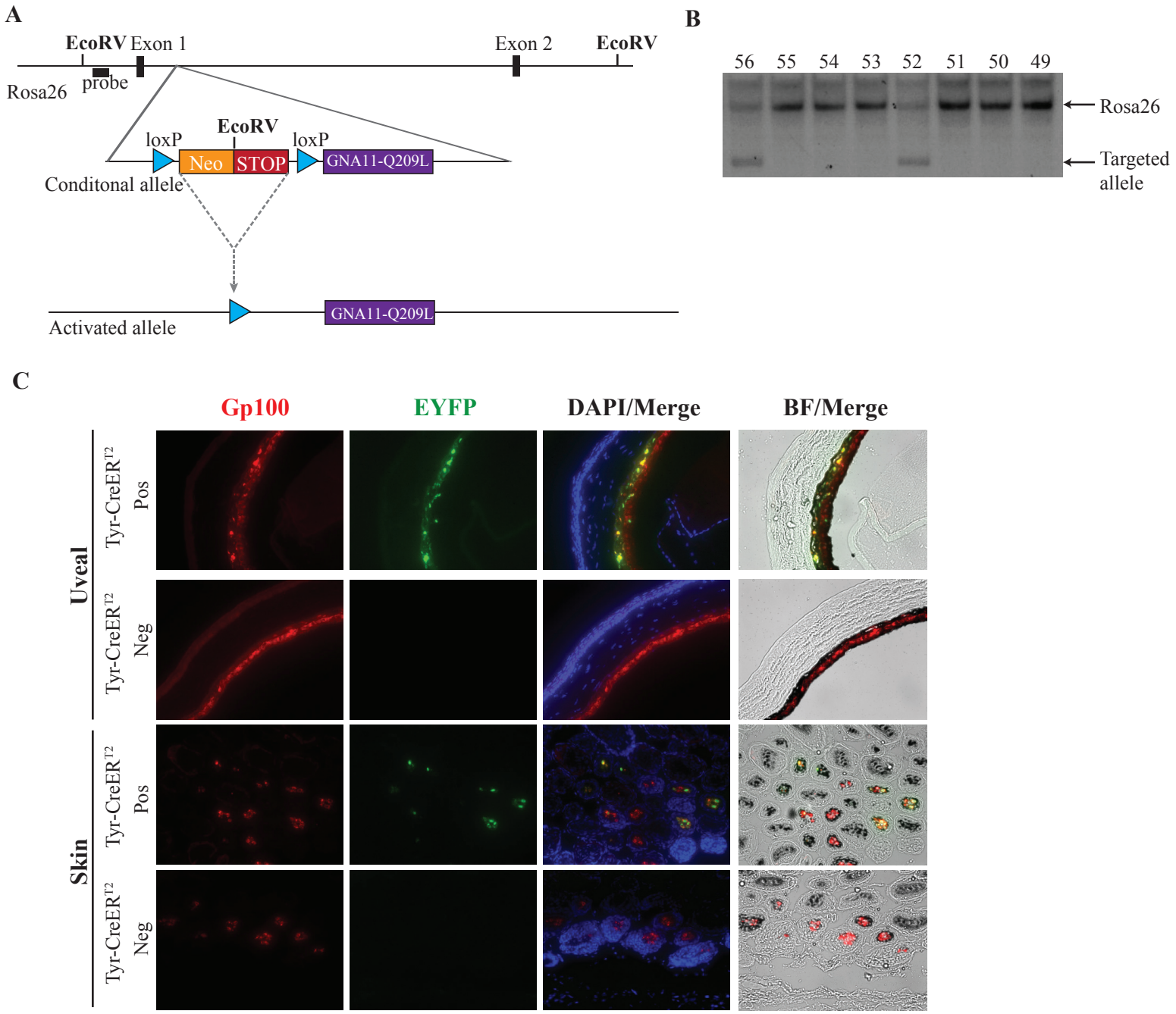

Figure S1, related to Figure 1. GNA11^{Q209L} mouse targeting

(**A**) Targeting strategy for conditional GNA11^{Q209L} allele in the *Rosa26* locus. Upon Cre-mediated recombination of the loxP, the Neo-STOP cassette is excised and GNA11^{Q209L} is expressed. Southern probe and *EcoRV* sites are indicated and targeting cassette introduces a new EcoRV site.

(**B**) Southern blot analysis using *EcoRV* and probing for 5'Rosa26. ES cell clones 56, 52 are positive for GNA11^{Q209L} allelic targetting.

(**C**) EYFP fluorescence, Gp100 immunofluorescence and bright-field images of uveal tract and skin in Tyr-CreER^{T2}; *CAG-LSL-EYFP* and control Cre-negative; *CAG-LSL-EYFP* mice 7 days after tamoxifen injection. Melanocytes are marked by Gp100-positivity as well as strong pigment readily appreciable on bright-field.

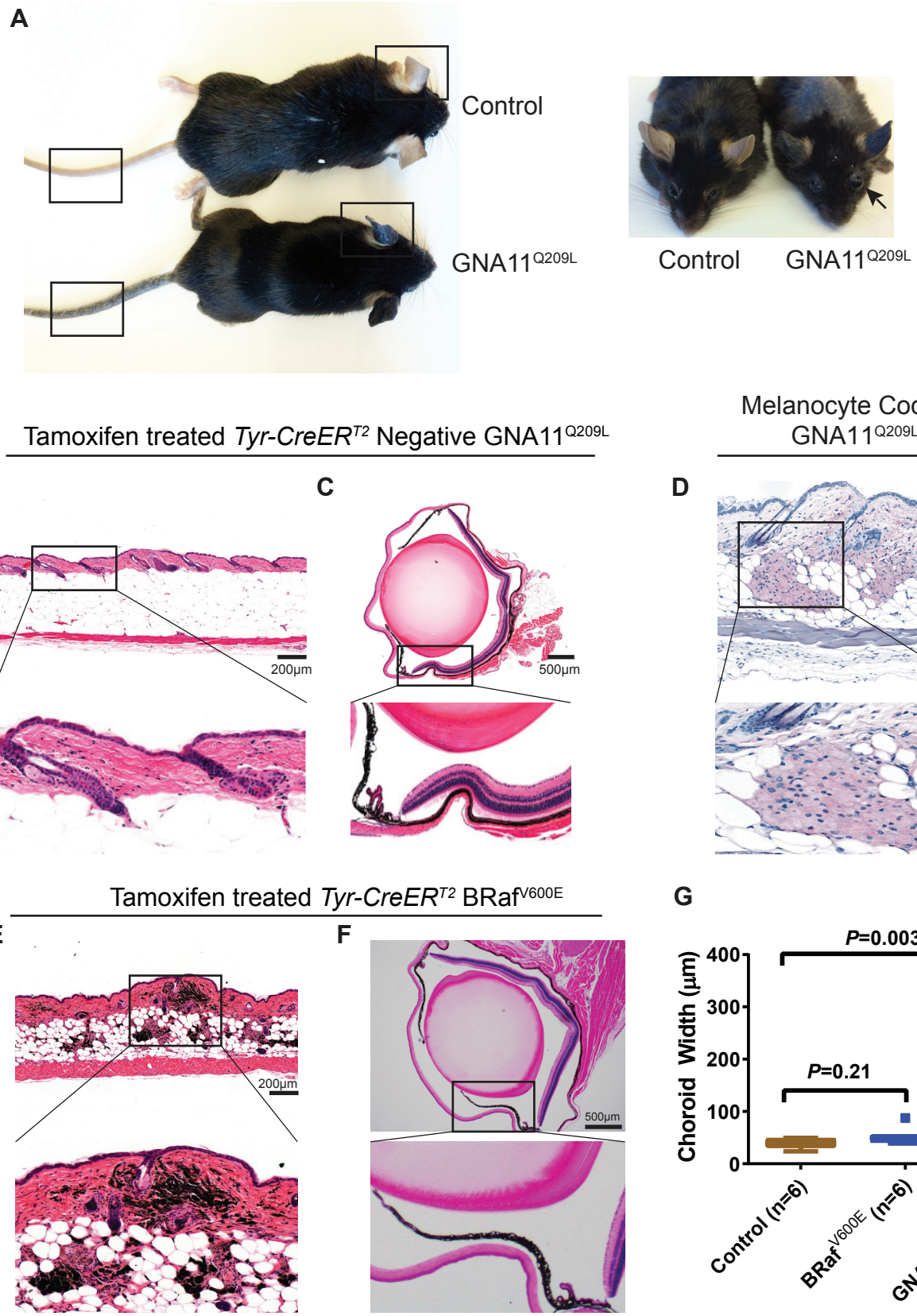

Figure S2, related to Figure 1. GNA11^{Q209L} and control mice phenotypes.

(**A**) Photographs of *Tyr-CreERT2* negative control and GNA11^{Q209L} mice 1 month after tamoxifen injection. Boxes highlight the pigmentation differences in the ears and tail. Arrow highlights the eye bulging.

(**B-C**) Representative H&E images of the skin (B) and eye (C) of a *Rosa26-LSL-GNA11^{Q209L}* (Cre-negative) mouse 12 months after tamoxifen injection.

(**D**) Immunohistochemistry of skin from a *Tyr-CreERT2; Rosa26-LSL-GNA11^{Q209L}* mouse 3 months after tamoxifen injection for melanoma cocktail (HMB45, DT101, BC199) using Red Chromogen (red) staining.

(**E-F**) Representative H&E images of the skin (**E**) and eye (**F**) of a 12-month tamoxifen treated BRaf^{V600E} mouse.

(**G**) Tukey plot of uveal width in mice of the indicated genotype 6 months after tamoxifen injection. Unpaired T-test.

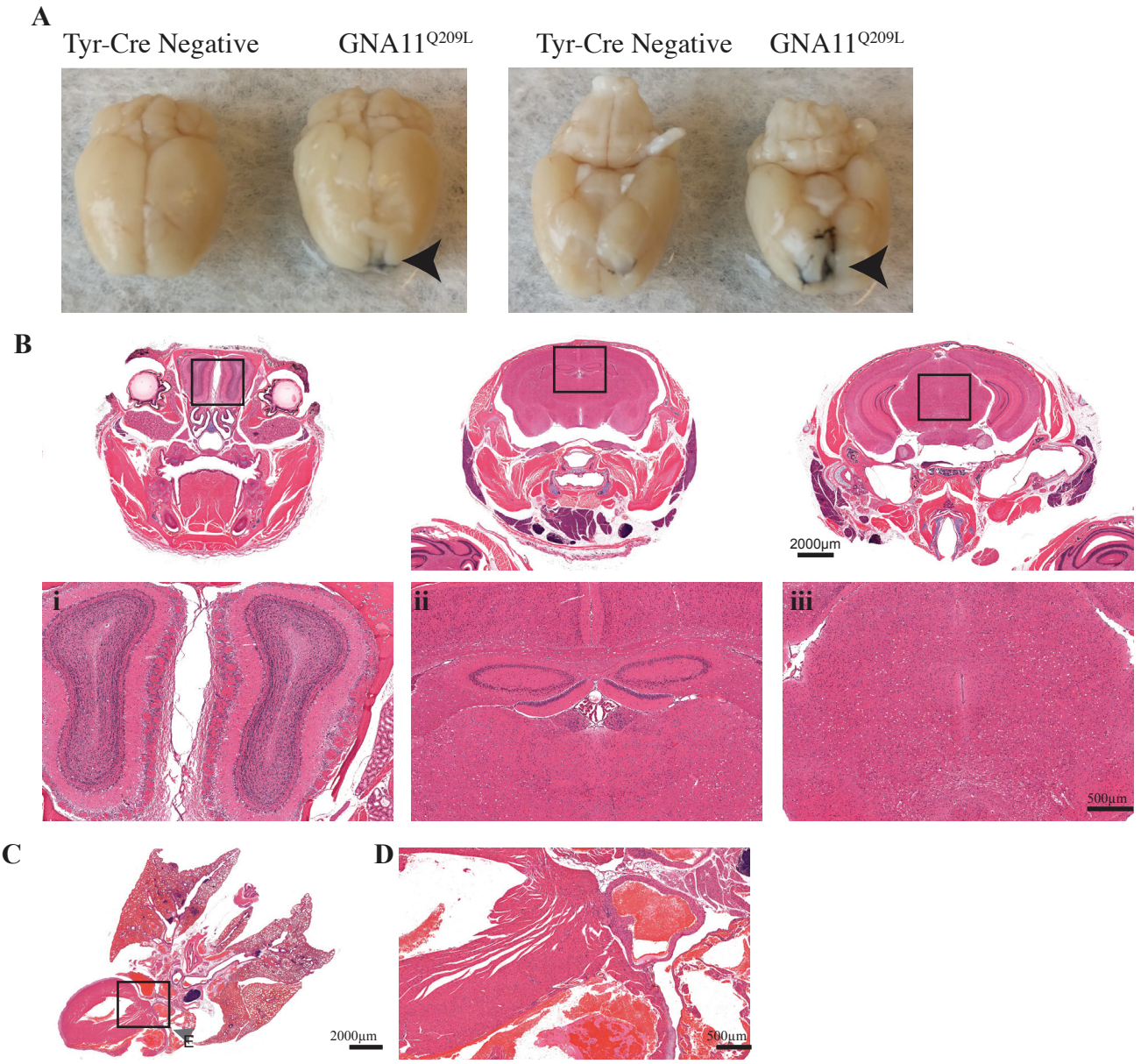

E

Months post-tamoxifen injection	<3	3-6	5-9	9+
$GNA11^{Q209L}$	1/4	8/8	4/4	2/2
Mean number of tumors (SD)	0.75 (1.5)	4.5 (2.6)	4.75 (2.6)	9.5 (3.5)
$GNA11^{Q209L}$ $Bap1^{KO}$	0/3	6/6	4/4	2/2
Mean number of tumors (SD)	0 (0)	3.8 (2)	4.25 (1.7)	8 (1.4)

Figure S3, related to Figures 2. $GNA11^{Q209L}$ CNS phenotype and controls.

(**A**) Representative images of whole brains showing focal pigmentation of the leptomeninges in $GNA11^{Q209L}$ (arrow).

(**B**) Sequential coronal skull sections (**top**), magnified images of select brain regions (**i**) olfactory bulb, (**ii**) choroid plexus of the third ventricle, (**iii**) meninges of the longitudinal fissure. Scale bar 2000µm (**top**), 500µm (**bottom**).

(**C**) Representative H&E image of heart and lung *Tyr-CreER^{T2}; BRaf^{V600E}* mice.

(**D**) Magnification of heart valve; box and gray arrowhead in (C). Scale bar 500µm.

(**E**) Prevalence of lung lesions in *Tyr-CreER^{T2}; R26-LSL-GNA11^{Q209L}* and *Tyr-CreER^{T2}; R26-LSL-GNA11^{Q209L}* mice by age post-tamoxifen injection.

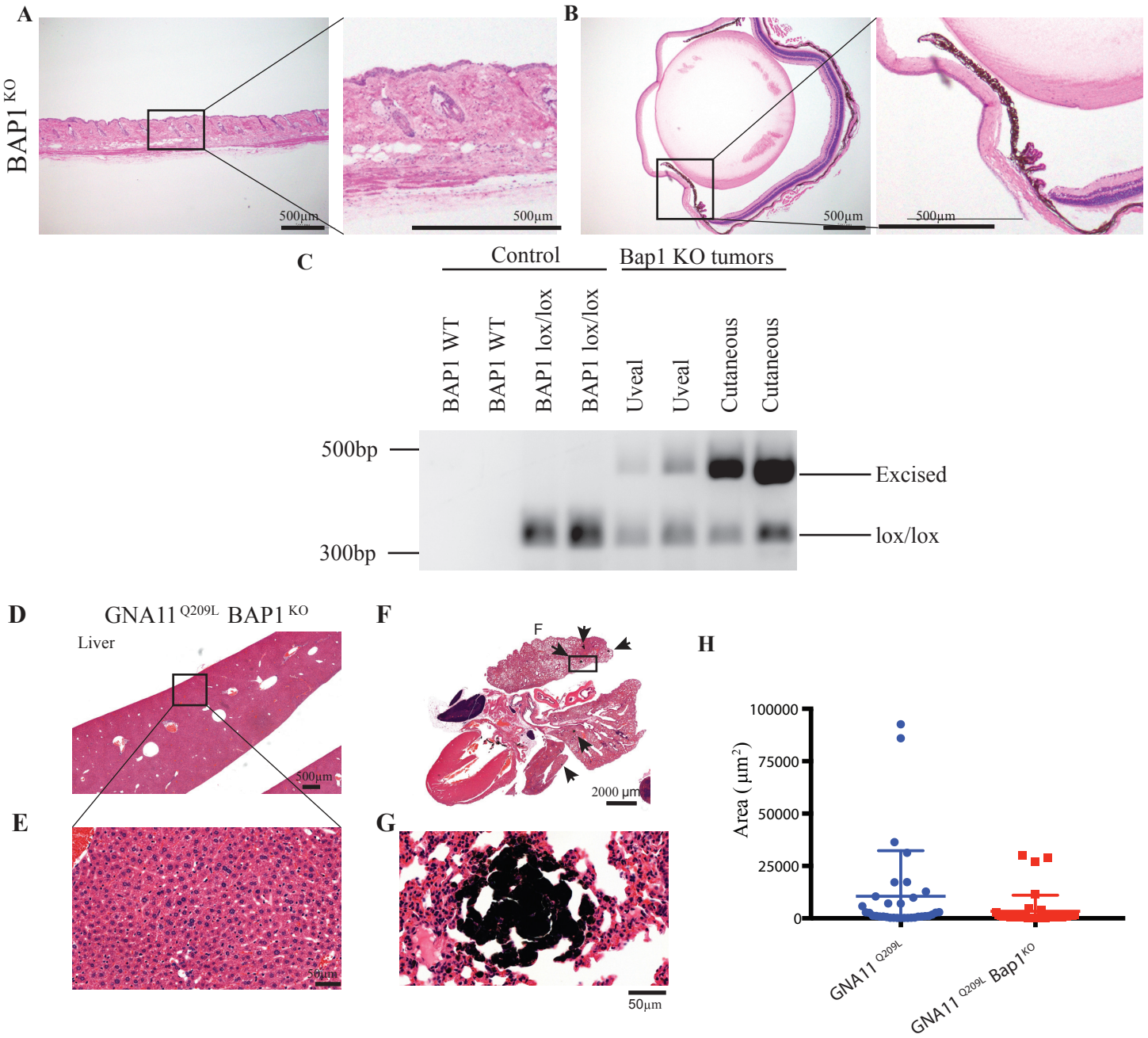

Figure S4, related to Figure 3. Bap1^{KO} mouse confirmation and histology

Representative H&E images of haired skin and subcutis (**A**) and eye (**B**) of *Tyr-CreER^{T2} Bap1^{KO}* mice 20-months post-tamoxifen injection. Scale bar 500µm.

(**C**) PCR for Bap1 lox/lox excision, controls and BAP1 KO tumors. Lox/lox amplification 327 bp and Bap1 KO (excision) 451 bp.

(**D-E**) Representative images of a GNA11^{Q209L} Bap1^{KO} mouse liver. Scale bar 500µm (D) and 50µm (E).

(**F**) Representative image of a GNA11^{Q209L} Bap1^{KO} mouse lung and heart. Scale bar 2000µm.

(**G**) Selected image of lung lesions. Image refers to box in (F). Scale bar 50 m.µ

(**H**) Quantification of lung tumor area (µm^2) in two mice per group (GNA11^{Q209L} and GNA11^{Q209L} Bap1^{KO}). Shown as scatter-dot plot; each dot represents the quantification of one tumor. Error bars; means ± s.e.m from all tumors present. *P* = ns.

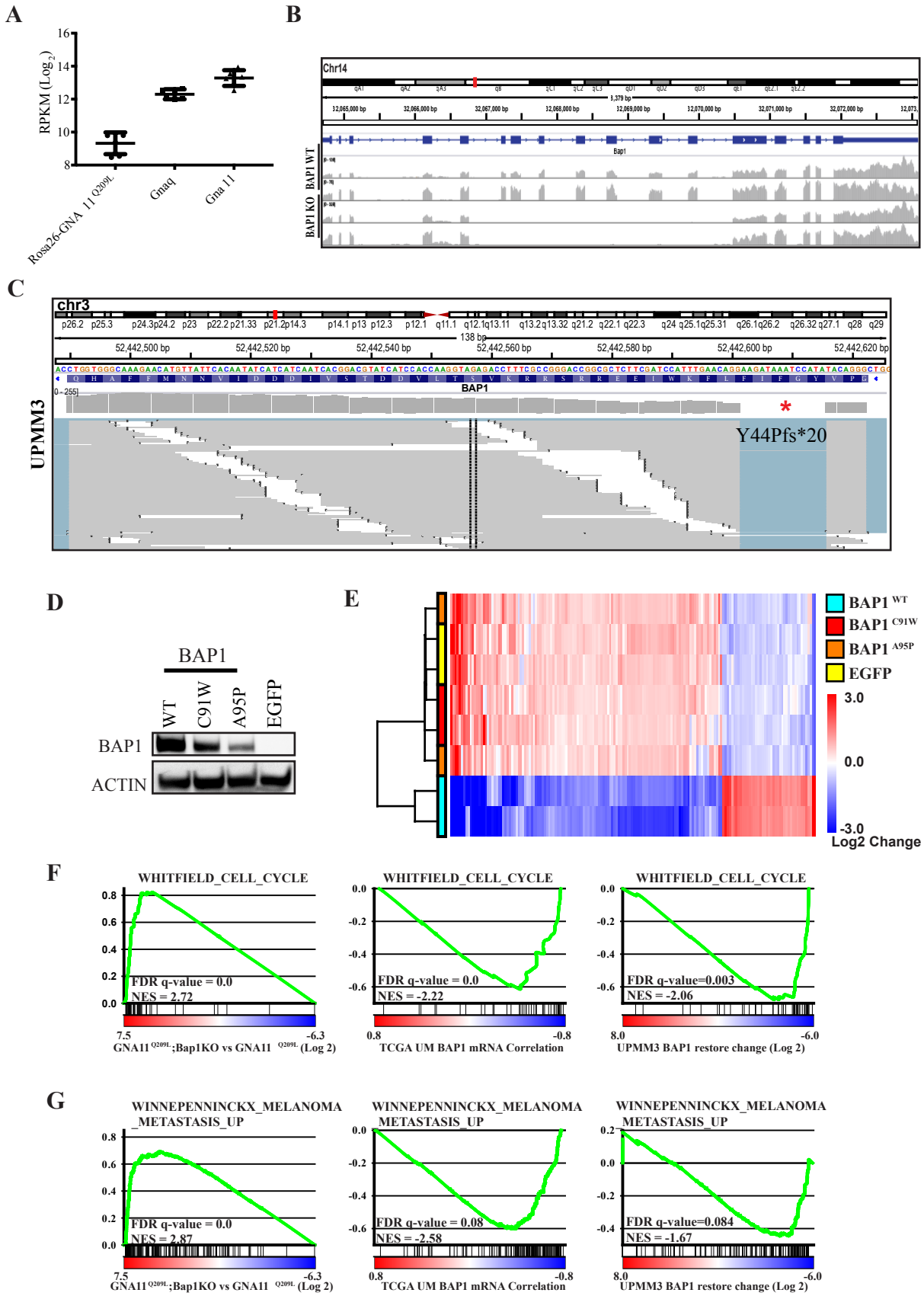

Figure S5, related to Figure 3. Bap1 RNA-sequencing reads in GNA11^{Q209L} tumors

(**A**) RNA-seq quantification of GNA11^{Q209L} positive mouse cutaneous tumors for Rosa26- GNA11^{Q209L} and endogenous *Gnaq* and *Gna11*. (**B**) Representative IGV view of RNA-seq reads at *Bap1* for GNA11^{Q209L} Bap1^{WT} and GNA11^{Q209L} Bap1^{KO} tumors showing deletion of exons 6-12. (**C**) IGV view of RNA-seq reads at *BAP1* for UPMM3 showing frameshift deletion (*). (**D**) Immunoblot of BAP1 for UPMM3 cells EGFP, BAP1 WT, BAP1 C91W and BAP1 A95P. (**E**) Hierarchial clustering of differential gene expression upon introduction of EGFP, BAP1 WT, BAP1 C91W and BAP1 A95P in duplicate. (**F**) Representative cell cycle signature (WHITFIELD_CELL_CYCLE) and (**G**) metastatic signature (WINNEPENNINCKX_MELANOMA_METASTASIS_UP) from GSEA analysis of each of three BAP1 datasets (mouse model, TCGA, and UPMM3 cell line).

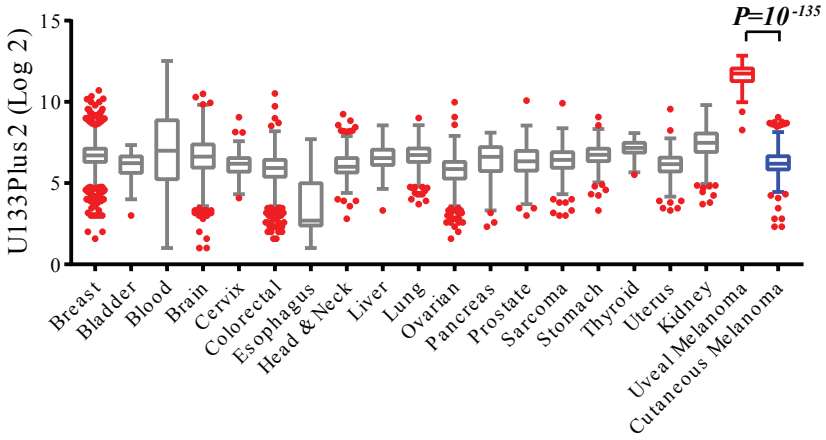

Figure S6, related to Figure 5. *RASGRP3* expression in Affymetrix U133Plus2 datasets

(**A**) Gene expression of *RASGRP3* across tumor types from the GENT (Gene Expression across Normal and Tumor tissue) U133Plus2 microarray database. Outliers shown in red dots. Uveal melanoma (red) and cutaneous melanoma (blue).

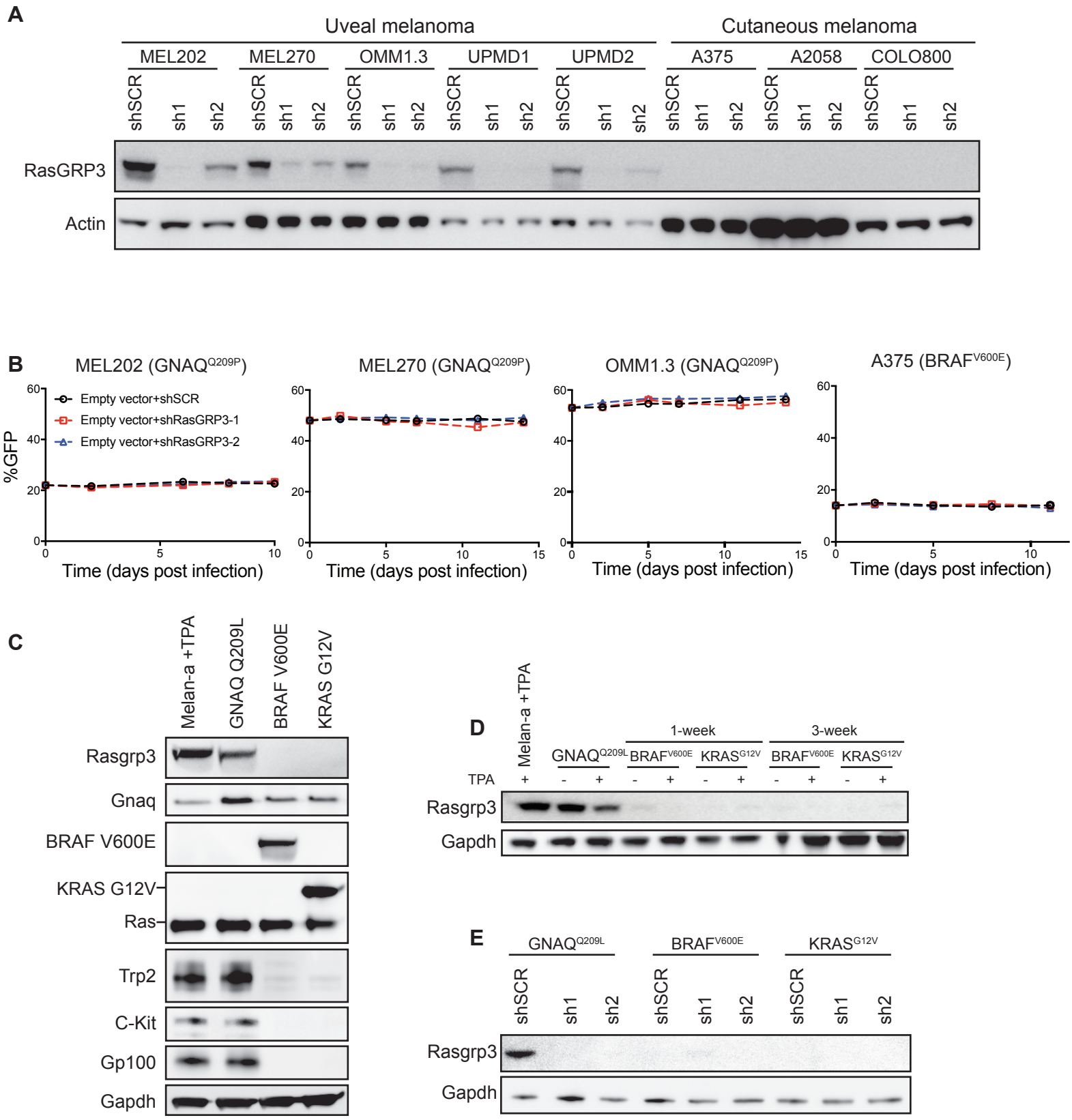

Figure S7, related to Figure 6 & 7. Depletion of RasGRP3 in panel of uveal and cutaneous melanoma cell lines
(A) Protein levels of RasGRP3 at day 3 of shRNA mediated knockdown of growth curve shown in Figure 6A-B. (**B**) Competition assay of empty vector-GFP rescue in the presence of RasGRP3 shRNA-mediated depletion. Uveal and cutaneous melanoma cells stably expressing doxycycline-inducible scrambled shRNA (shSCR) or shRNA targeting RASGRP3 (shRASGRP3-1, shRASGRP3-2) in the presence of KRASG12V-GFP. Percentage of GFP analyzed via flow cytometry over time.(**C**) Protein levels of RasGRP3 and melanocyte makers (Trp2, C-Kit and Gp100) in transduced melan-a cells with GNAQ^{Q209L}, BRAF^{V600E} and KRAS^{G12V}. (**D**) Protein levels of RasGRP3 by immunoblot at upon addition of TPA to the media of GNAQ^{Q209L}, BRAF^{V600E} and KRAS^{G12V} cells for 1- and 3-weeks, respectively. (**E**) Protein levels of RasGRP3 by immunoblot at day 3 of shRNA mediated knockdown of Rasgrp3 corresponding to the growth curve shown in Figure 7A

Table S2. Mouse genotyping primers and Quickchange primers. Related to Figures 1-3, 6-7.

Genotype primer	**Forward**	**Reverse**	**Additonal**
Tyr-Cre	CAGGGTGTTATAAGCAATCCC	CCTGGAAAATGCTTCTGTCCG	
Bap1 lox/lox	CCACAACGGGTTCTTCTGTT	ACTGCAGCAATGTGGATCTG	GAAAAGGTCTGACCCAGATCA
BRAF CA	TGAGTATTTTTGTGGCAACTGC	CTCTGCTGGGAAAGCGGC	
GNA11 Q290L	CGTGGAGAAGGTGACCACC	GATCCACTTCCTCCGCTC	
Rosa26	TCCCGACAAAACCGAAAATC	AAGCACGTT TCCGACTTGAG	
Quikchange primer	**Forward**	**Reverse**	
BRAF V600E	ccactccatcgagatttctctgtagctagaccaaaat	attttggtctagctacagagaaatctcgatggagtgg	
GNAQ Q209L	cttctctctgaccttaggccccctacatcga	tcgatgtaggggcctaaggtcagagagaag	
BAP1 excision primer	**Forward**	**Reverse**	
Bap1 KO	GCCACTGCATGGTATCTGGT	CAGGTGGCCTCCTCTACTCT	TCTTTTCCGCCTACTGCGAC

Table S3. shRNA sequences and RNAi Consortium ShRNA Library numbers. Related to Figures 6-7.

	Sequene	**The RNAi Consortium ShRNA Library #**
Human shRASGRP3-1	GCTGCAATGAATTTCGATTAA	TRCN0000048113
Human shRASGRP3-2	GCCTCAGTCATAGTTCCATTT	TRCN0000048114
Mouse shRasgrp3-1	GCCTGCCTCTTATTTGACCAT	TRCN0000022732
Mouse shRasgrp3-2	GCTGGTGTGGATGTTGTAGAT	TRCN0000022733